Active Fault Tolerant Control of Grid-Connected DER: Diagnosis and Reconfiguration

Behnam Khaki
Smart Grid Energy Research Center
Department of Mechanical Engineering
University of California
Los Angeles, California 90095
Email: behnamkhaki@ucla.edu

Heybet Kiliç
Department of Electric
Power and Energy
Dicle University
Diyarbakir, Turkey 21280
Email: heybet.kilic@dicle.edu.tr

Musa Yilmaz
Department of Electronics and
Telecommunication Engineering
Batman University
Batman, Turkey 72100
Email: musa.yilmaz@batman.edu.tr

Miadreza Shafie-khah
School of Technology and Innovations
University of Vaasa
65200 Vaasa, Finland
Email: miadreza@gmail.com

Mohamed Lotfi, João P. S. Catalão
Faculty of Engineering
University of Porto and INESC TEC
Porto 4200-465, Portugal
Emails: mohd.f.lotfi@gmail.com, catalao@fe.up.pt

***Abstract*—In this paper, we propose an active fault tolerant control (FTC) to regulate the active and reactive output powers of a voltage source converter (VSC) in the case of actuator failure. The active fault tolerant controller of the VSC which connects a distributed energy resource to the distribution power grid is achieved through the fault diagnostic and controller reconfiguration units. The diagnostic unit reveals the actuator failure by comparing the known inputs and measured outputs of VSC with those of the faultless model of the system and testing their consistency. In the case of actuator failure, the reconfiguration unit adapts the controller to the faulty system which enables the VSC to track the desired active and reactive output powers. The reconfiguration unit is designed using the virtual actuator which does not interfere with the regular controller of the VSC. The effectiveness of the proposed active FTC is evaluated by the numerical simulation of a VSC connected to the AC distribution grid.**

***Index Terms*—Voltage source converter, grid-connected distributed energy resource, fault diagnosis, virtual actuator.**

I. Introduction

Conventional power grids with top-down structure rely on the large fossil fuel-based power stations emitting CO_2. Also, they are experiencing considerable power loss, voltage fluctuation, and feeder congestion due to increasing load demand. To overcome these issues, distributed energy resources (DERs) with efficient power electronic converters can be deployed [1]- [3], as they are mostly based on renewable energies (such as solar, wind, and fuel cell) and located close to the electricity consumers. DER deployment can also increase load reliability as in the case of power outage, the load demands can be satisfied through the operation of DERs in islanded mode. Nevertheless, inherent intermittency and uncertainty of output power are considered the main disadvantages of DERs [4]. The solution is the controller for the power electronic interfaces of DERs which is robust against the faults in sensors and actuators, and it and can drive DER output power toward the desired value. The focus of this paper is to design an active fault-tolerant control (FTC) consisting of diagnosis and and reconfiguration units.

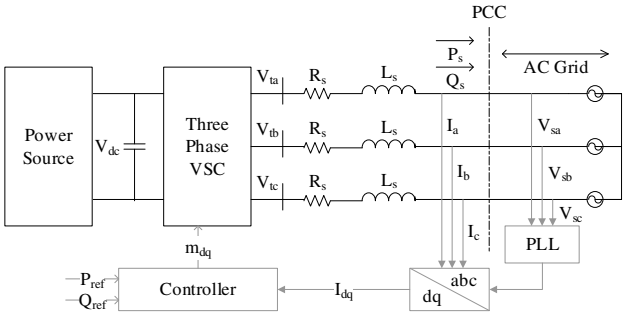

Fig. 1. Schematic diagram of grid-connected DER.

Although a variety of methods have been proposed for fault detection, isolation, and tolerance in DERs and power grids [5]- [12], there are a few studies on a comprehensive actuator fault detection and controller reconfiguration. Most of the present studies are on the short circuit and sensor faults detection [5]- [7]. As some cases in point, two sensor fault detection methods, which are observer-based, for power system load frequency control loops are presented in [8]- [9]. In [10]- [11], the authors propose an observer-based fault tolerant control method for the sensor fault in the DERs. Also, a virtual actuator (VA) based FTC method for wide-are control of power systems is investigated in [12], and a model based framework to estimate and accommodate the actuator fault in a solid oxide fuel cell is proposed in [13]. In the former research, the authors do not provide any fault estimation approach, and in the latter, the authors design a controller working based on a switching rule to accommodate actuator failure.

To address the lack of a comprehensive actuator fault detection and control reconfiguration for DERs, a VA-based

978-1-7281-4878-6/19/$31.00 ©2019 IEEE

active FTC approach [14] is proposed in this paper. The proposed FTC approach consists of two parts: an observer-based diagnostic unit which compares the known input and measured output signals of the plant to check their consistency with the faultless model of the plant; and a reconfiguration unit which is used to satisfy the desired performance of the faulty plant by adapting the controller. In the proposed method, the reconfiguration unit is based on the fault hiding principal [15], in which VA is inserted between the ordinary output feedback controller of the DER and the faulty plant, and it is triggered if the actuator failure is detected by diagnostic unit. In this way, the plant is reconfigured so that the fault is hidden from the nominal controller, and the output powers of the faulty VSC is (approximately) similar to the faultless system.

The structure of this paper is organized as follows: DER dynamic model in *dq* frame and its nominal output feedback controller are introduced in Section II; diagnosis and reconfiguration units of the proposed FTC are presented in Section III; the implementation of the proposed active FTC for the DER and its performance evaluation are performed in Section IV by numerical simulations; and finally, the paper is concluded in Section V.

II. DER Modeling and Control

In this section, the mathematical model of the DER and its output feedback controller are presented. The electrical diagram of a DER is shown in Fig. 1, in which a three-phase voltage source converter (VSC) and a series RL branch connect the DC source to the AC grid. The RL branch is the filter reducing the high-frequency harmonics of the AC current. The dynamic model of VSC on the AC side is as follows:

$$L\frac{d\vec{i}(t)}{dt} = L_s\omega_0 i - R_s\vec{i}(t) + \vec{v}_t - \vec{v}_s, \tag{1}$$

where $\vec{i} = i_{dq}e^{j\rho(t)}$ is the output current of VSC, $\vec{v}_t = v_{t_{dq}}e^{j\rho(t)}$ is the terminal voltage of VSC, and $\vec{v}_s = v_{s_{dq}}e^{j\rho(t)}$ is the voltage of VSC at the point of common coupling (PCC). Using the phase-locked loop (PLL) ensures that $v_{s_q} = 0$ and $\rho = (\omega_0 t + \theta_0)$. Therefore, the dynamics of DER in *dq* frame are governed by:

$$\begin{aligned} L\frac{di_d}{dt} &= L_s\omega_0 i_q - R_s i_q + v_{td} - v_{sd} \\ L\frac{di_q}{dt} &= -L_s\omega_0 i_d - R_s i_d + v_{tq}, \end{aligned} \tag{2}$$

in which L_s is the inductance of the filter, and R_s represents the ohmic loss of the filter and converter. *dq* components of v_t are:

$$\begin{aligned} v_{td} &= \frac{v_{DC}}{2}m_d(t) \\ v_{tq} &= \frac{v_{DC}}{2}m_q(t), \end{aligned} \tag{3}$$

where m_d and m_q denote, respectively, the d and q components of the Pulse Width Modulation (PWM) signal which regulates the output current of VSC.

Equation (2) can be rewritten as the state-space model of a linear time invariant system, i.e.

$$\Sigma : \begin{cases} \dot{x}(t) = Ax(t) + Bu(t) + Dw(t) \\ y(t) = Cx(t), \end{cases} \tag{4}$$

where $x = [i_d\ i_q]^T \in \mathbb{R}^2$ is the state vector, $u = [m_d\ m_q]^T \in \mathbb{R}^2$ is the input or control vector, $w = [v_{sd}\ v_{sq}]^T \in \mathbb{R}^2$ is the disturbance vector, and $y \in \mathbb{R}^2$ is the output vector of the system. The system matrices, i.e. A, B, C, and D, are:

$$\begin{aligned} A &= \begin{bmatrix} -\frac{R_s}{L_s} & \omega_0 \\ -\omega_0 & -\frac{R_s}{L_s} \end{bmatrix}, \qquad B = \begin{bmatrix} \frac{1}{L_s} & 0 \\ 0 & \frac{1}{L_s} \end{bmatrix} \\ C &= \begin{bmatrix} 1 & 0 \\ 0 & 1 \end{bmatrix}, \qquad D = -B. \end{aligned} \tag{5}$$

The primary objective of DER controller is to regulate the active and reactive powers exchanged with the distribution grid at PCC according to the reference values determined by the grid operator. The exchanged active (P_s) and reactive (Q_s) powers at PCC are represented in the *dq* frame as:

$$P_s(t) = \frac{3}{2}(v_{s_d}i_d + v_{s_q}i_q) \tag{6a}$$

$$Q_s(t) = \frac{3}{2}(-v_{s_d}i_q + v_{s_q}i_d). \tag{6b}$$

Considering the fact that $v_{sq} = 0$ and using (6), the reference values for i_d and i_q can be expressed as:

$$i_{d_{ref}} = \frac{2}{3v_{s_d}}\left(P_{s_{ref}}\right) \tag{7a}$$

$$i_{q_{ref}} = \frac{-2}{3v_{s_d}}\left(Q_{s_{ref}}\right), \tag{7b}$$

where $P_{s_{ref}}$ and $Q_{s_{ref}}$ are the desired active and reactive powers, respectively, defined by the grid operator.

It can be shown that the system Σ (4) is controllable as well as observable. Thus, the following output feedback controller can move the system states toward the desired trajectory.

$$u = Ky, \tag{8}$$

where K is the controller gain which ensures asymptotic stability of the system.

III. Fault-Tolerant Controller with Virtual Actuator

The primary goal of the active FTC is to keep the system stable and its power output equal to the desired value while the system is experiencing actuator failure. The proposed FTC shown in Fig. 2 consists of the following units[1]:

1) Observed-based diagnostic unit.
2) VA-based reconfiguration unit.

The observed-based diagnostic unit compares the known input of the controller and measured output of DER to calculate the residuals. In the case of actuator fault, the reconfiguration unit modifies the controller by a VA to ensure the system stability

[1]For more details refer to [14]

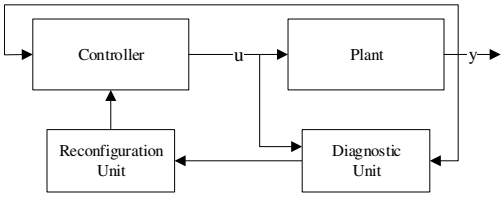

Fig. 2. Block diagram of the system with active FTC controller.

and its desired operation. The FTC is added to the nominal controller loop as shown in Fig. 2, and the fault diagnosis and reconfiguration units modify controller and construct a closed-loop to keep system in operation when actuator fault is detected.

We define $\mathcal{F}$ as the set of actuator faults. The aim of this section are to identify the actuator fault $f \in \mathcal{F}$ which changes the dynamic behavior of the system Σ (4), and to reconfigure the controller so that the system follows the desired steady state trajectory under faulty condition. The model of the faulty system Σ is presented by:

$$\Sigma_f : \begin{cases} \dot{x}(t) = A_f x(t) + B_f u(t) \\ y(t) = C_f x(t). \end{cases} \tag{9}$$

The paper primarily focuses on the actuator faults which change only the B matrix of Σ to B_f. The diagnostic unit designed in the following should be able to determine if the system is faultless or experiencing actuator faulty conditions. In addition, the diagnostic unit's performance should not depend on the type of the system regular controller. In the case of faulty actuator and through the reconfiguration mode, the nominal controller of DER remains in the control loop, so the proposed active FTC is independent of the controller type.

A. Structural Fault Diagnosis

To make the fault detection possible, the information about the system Σ must include redundancies. In the following, it is shown how such redundancies are found for a bipartite structure graph.

For the structural analysis, the model Σ for $u(t) = 0$ is interpreted as

$$\Sigma : \begin{cases} e_1 : \dot{x}_1(t) = a_{11}x_1(t) + ... + a_{1n}x_n(t) \\ \quad . \\ \quad . \\ \quad . \\ e_n : \dot{x}_n(t) = a_{n1}x_n(t) + ... + a_{nn}x_n(t) \\ m_1 : y_1(t) = c_{11}x_1(t) + ... + c_{1n}x_n(t) \\ \quad . \\ \quad . \\ \quad . \\ m_p : y_p(t) = c_{p1}x_1(t) + ... + c_{pn}x_n(t) \\ d_i : \dot{x}_i(t) = \dfrac{d}{dt}x_i(t), \ i = 1, ..., n, \end{cases} \tag{10}$$

where e_i $(i = 1, ..., n)$, m_i $(i = 1, ..., p)$ and d_i $(i = 1, ..., n)$ stand for the state equations, the output equations, and the differential constraints, respectively. We define the set $\mathcal{C}$ of constraints describing the behavior of Σ as follows:

$$\mathcal{C} = \{d_1, ..., d_n, e_1, ..., e_n, m_1, ..., m_p\}.$$

The elements of the set $\mathcal{Z}$ are the signals appearing in those constraints:

$$\mathcal{Z} = \{\dot{x}_1, ..., \dot{x}_n, x_1, ..., x_n, y_1, ..., y_p\},$$

where the unknown and known signals are shown by $\mathcal{X}_*$ and $\dot{\mathcal{X}}$, respectively, as follows

$$\mathcal{X}_* = \{x_1, ..., x_n\}, \quad \dot{\mathcal{X}} = \{\dot{x}_1, ..., \dot{x}_n\}.$$

For the set of equality constraints $\mathcal{C}$,

$$\text{var}(c) := \{z \in \mathcal{X} | z \text{ emerges in an equation } c \in \mathcal{C}\}.$$

For the $c \subset \mathcal{C}$, $\text{var}(c)$ indicates the set of variables in the equation of c, consisting of known, unknown, and fault variables [16].

The structural model of (4) can be presented as a bipartite graph by:

$$\mathcal{G} = (\mathcal{C}, \mathcal{Z}, \mathcal{E}).$$

The vertices of the set $\mathcal{C}$ are labeled by d_i, e_i, and m_i of the constraints, while the elements of the set $\mathcal{Z}$ are indicated by the names of the signals. The set of edges $\mathcal{E} \subseteq \mathcal{C} \times \mathcal{Z}$ is presented as [14]:

$$(c_i, z_i \in \mathcal{E}) \text{ if } z_j \in \text{var}(\{c_i\}).$$

The purpose of analyzing bipartite graph is to identify over-determined subsets of the equality constraints in (10) which include more equations than the unknowns. Those subsets are the candidates for residual generation in diagnostic unit.

The incidence matrix G of bipartite graph is created to identify over-determined subsets $\mathcal{G}^+ = (\mathcal{C}^+, \mathcal{X}^+, \mathcal{E}^+)$. A "1" in the intersection of row c_i and column z_j in G means that the edge $(c_i, z_j) \in \mathcal{E}$ exists. If the value in the intersection is equal to zero, it means that there is no edge between c_i and z_j. The incidence matrix for the system (10) can be constructed as below:

$G =$

	$\dot{x}_1$ . . . $\dot{x}_n$	x_1 . . . x_n
d_1	①	1
.	.	.
.	.	.
.	.	.
d_n	①	1
e_1	1	
.	.	
.	.	$[A]$
.	.	
e_n	1	
m_1		
.		
.	O	$[C]$
.		
m_p		

The DULMAGE-MENDELSOHN decomposition (DM decomposition) is used to turn the structure graph into three subgraphs as follows:

$$\begin{aligned}\mathcal{G}^- &= \left(\mathcal{C}^-, \mathcal{X}^-, \mathcal{E}^-\right)\\ \mathcal{G}^0 &= \left(\mathcal{C}^0, \mathcal{X}^0, \mathcal{E}^0\right)\\ \mathcal{G}^+ &= \left(\mathcal{C}^+, \mathcal{X}^+, \mathcal{E}^+\right),\end{aligned}$$

where $\mathcal{X} = \mathcal{X}^+ \cup \mathcal{X}^0 \cup \mathcal{X}^-$, $\mathcal{C} = \mathcal{C}^+ \cup \mathcal{C}^0 \cup \mathcal{C}^-$ and $\mid \mathcal{C}^- \mid < \mid \mathcal{X}^- \mid$, $\mid \mathcal{C}^0 \mid = \mid \mathcal{X}^0 \mid$, $\mid \mathcal{C}^+ \mid > \mid \mathcal{X}^+ \mid$. The subset $\mathcal{C}^+$ is structurally over-determined, and it also provides redundancy which is important for fault diagnosis.

If the set $\mathcal{C}^+$ consists of every state variable $x_i \in \mathcal{X}^+$ the state equation e_i, the fault diagnosable subsystem of (9) is represented by:

$$\Sigma^+ : \begin{cases}\dot{x}^+(t) = A^+ x^+(t) + B^+ u(t)\\ y^+(t) = C^+ x^+(t).\end{cases} \tag{11}$$

Any fault $f \in \mathcal{F}$ altering a single constraint $c \in \mathcal{C}$ is represented as $c(f)$. $f \in \mathcal{F}$ will be called structurally faulty-detectable if it belongs to the over-determined subset $c(f) \in \mathcal{C}^+$. The set of detectable faults is defined by $\mathcal{F}^+$ as follows

$$\mathcal{F}^+ = \left\{ f \in \mathcal{F} | c(f) \in \mathcal{C}^+ \right\}.$$

B. Observer-Based Residual Generation for Fault Detection

As mentioned in the preceding subsection, the over-determined set $\mathcal{C}^+$ is known as structurally diagnosable part of the system (9). Using the set $\mathcal{C}^+$, analytical redundancy relation (ARR) is defined as:

$$r(t) = g(u(t), \dot{u}(t), \ddot{u}(t), ..., y(t), \dot{y}t(t), \ddot{y}(t), ...), \tag{12}$$

which includes the known input and measured output signals and their derivatives. The function $r(t)$ is solved to obtain the residuals. In practice, however, it is difficult to obtain the residuals as the derivatives can not be measured. Therefore, an observed-based diagnostic method is used to obtain the residuals, which is realized through two steps: fault detection and fault isolation. The fault detection part utilizes the detector observer

$$\Sigma_D : \begin{cases}\dot{\hat{x}}(t) = A_\delta \hat{x}(t) + Bu(t) + Ly(t)\\ \hat{r}(t) = C\hat{x}(t) - y(t),\end{cases} \tag{13}$$

where $A_\delta = A - LC$. The matrix L is chosen such that matrix A_δ is asymptotically stable. In the case of faultless system, this observer has a vanishing residual ($r(t) = 0$). If an actuator fault occurs, residual will be greater than zero (or a specific threshold), i.e. $\lim_{t\to\infty} ||r(t)|| \neq 0$.

C. Reconfiguration of Controller and Virtual Actuator

The reconfigurable controller considered in this paper ensures fault-hiding principle from the perspective of the control unit. A reconfigurable block which consists of a VA is placed between the regular control unit and the faulty system, without changing the nominal controller. This results in the fact that the reconfiguration block can be constructed by comparing the behavior of the nominal plant and the reconfigured plant, without any knowledge about the nominal controller. The schematic diagram of the reconfigurable block is shown in Fig. 3. The goal is to design a reconfigurable block which makes the behavior of the reconfigured plant similar to the nominal plant, and it hides the fault from the regular controller unit.

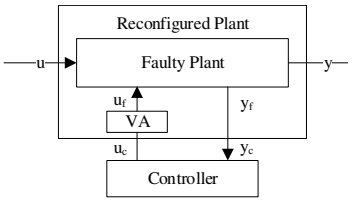

Fig. 3. VA located between the nominal controller and the faulty system.

The VA is shown by the following state-space model

$$\Sigma_{VA} : \begin{cases}\dot{\hat{x}}_\Delta(t) = A_\Delta \hat{x}_\Delta(t) + B_\Delta u_c(t)\\ u_f(t) = M x_\Delta(t) + N u_c(t)\\ y_c(t) = C x_\Delta(t) + y_f(t),\end{cases} \tag{14}$$

where $A_\Delta = A - B_f M$, $B_\Delta = B - B_f N$. The matrices M and N are designed to achieve a quick transient response for the reconfigured closed-loop system. The following conditions should be satisfied to design the VA, which is the reconfiguration block in the case of the actuator faults.

- Reconfigurable block should ensure that $y_c(t) = y_f(t)$.
- The reconfigured plant should follow the trajectory $x_c(t) = x_f(t)$.

Particularly, I/O trajectory recovery, $y_c(t) = y_f(t)$, and state recovery, $x_c(t) = x_f(t)$, can be accomplished if the following equation is satisfied:

$$rank(B_f) = rank(B\ B_f).$$

Then the VA (Σ_{VA}) reduces to a static system as:

$$u_f(t) = N u_c(t). \tag{15}$$

where $N = B_f^+ B$, and $(.)^+$ indicates the pseudoinverse matrix.

IV. Numerical Simulation & Results

To evaluate the performance of the designed active FTC, the DER connected to the AC grid (Fig. 1) is simulated on MATLAB. The parameter values of the DER are shown in Table I. $f_0 = 2\pi/\omega_0$ is the nominal power frequency of the AC grid which has the Line-to-Line voltage of $V_{rms} = 480V$ and a system frequency of $f_0 = 60$ Hz. It is also assumed that the DER is capable of supplying the desired active (P_{ref}) and reactive (Q_{ref}) powers determined by the grid.

At the beginning of the simulation ($t \in [0, 0.15)$ sec), the circuit breaker of VSC is open, and it is disconnected from the grid. The voltage fluctuations over this time period in Fig. 4 show that PLL reaches steady state condition. Afterwards ($t \in [0.15, 0.2)$ sec), VSC is connected to the grid, but $P_{ref} =$

TABLE I
PARAMETER VALUES OF THE SIMULATED DER.

Parameter	L_s	R_s	V_{DC}	$v_{s_{rms}}$	f_0
value	$100\mu H$	$1.63m\Omega$	$125VDC$	$480VAC$	$60Hz$

0 and $Q_{ref} = 0$. While Q_{ref} is still zero, over the period $t \in [0.2, 0.3)$ sec, $P_{ref} = 0.2$ MW, and for $t \geq 0.3$ sec, $P_{ref} = -0.2$ MW. Q_{ref} is equal to 0.5 MVar for $t \geq 0.35$ sec. Following the reference values of active and reactive powers by the DER is shown in Fig. 5, and the current dynamics are illustrated in Fig. 6.

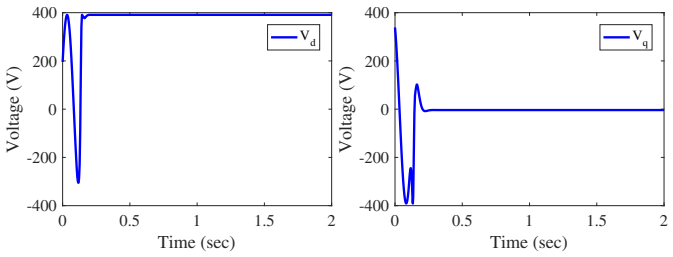

Fig. 4. Output voltage of DER on d (left) and q (right) axes.

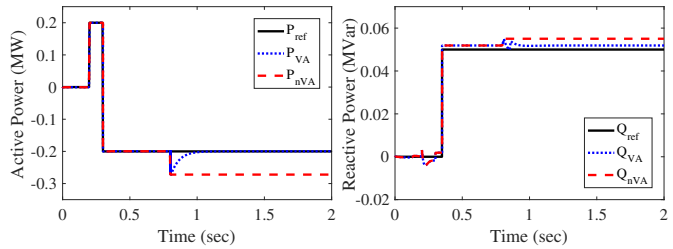

Fig. 5. Output active (left) and reactive (right) powers of DER with/out VA.

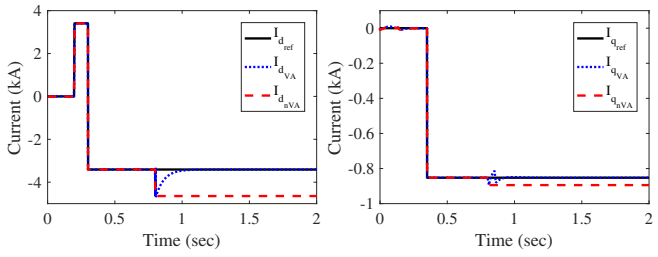

Fig. 6. Output current of DER on d (left) and q (right) axes with/out VA.

As shown in Fig. 5 and Fig. 6, system outputs are in the steady state when a fault occurs at 0.8 sec. It is obvious in Fig. 7 that both residuals are zero before the actuator failure. When the failure happens, residuals exceed the threshold value of zero, so the designed observer identifies the residuals' increase as a fault, and the reconfiguration unit by VA is activated to keep the system outputs equal or close to the desired values. As the error between DER active and reactive power outputs and the corresponding reference values decreases, the residuals decrease to zero. In the figures, q and d subscripts stand for q and d axes components, ref is the reference value, VA shows the result with VA-based controller, and nVA is for the results without VA-based controller.

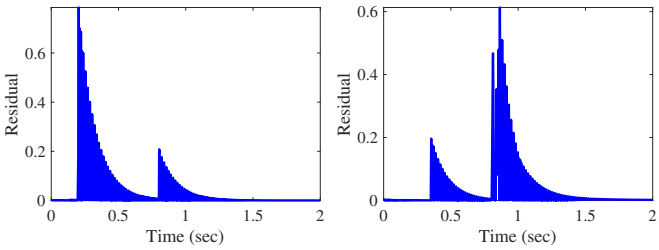

Fig. 7. Residuals on d (left) and q (right) axes with VA.

V. CONCLUSION & FUTURE WORK

In this paper, an active FTC was designed for a grid-connected DER. The proposed active FTC includes the observer-based fault diagnostic unit and the VA-based reconfiguration unit. The diagnostic unit identifies the failure in DER actuator using the *dq* components of observer residuals, and the reconfiguration unit reconfigures the faulty plant using VA so that the fault remains hidden for the regular controller of the DER. The effectiveness of the active FTC was shown by simulation of a grid-connected DER. As the future work, we will design a virtual sensor (VS) for the case of sensor failure, and evaluate the performance of the designed VA and VS for a grid-connected microgrid.

ACKNOWLEDGMENTS

M. Lotfi and J.P.S. Catalão acknowledge the support by FEDER funds through COMPETE 2020 and by Portuguese funds through FCT, under 02/SAICT/2017 (POCI-01-0145-FEDER-029803).

REFERENCES

[1] D. Olivares, A. Mehrizi-Sani, A. Etemadi, C. Canizares, R. Iravani, M. Kazerani, A. Hajimiragha, O. Gomis-Bellmunt, M. Saeedifard, R. Palma-Behnke, G. Jimenez-Estevez, and N. Hatziargyriou, "Trends in microgrid control," *IEEE Trans. Smart Grid*, vol. 5, no. 4, pp. 198–205, Jul. 2014.

[2] H. A. Rahman, M. S. Majid, A. R. Jordehi, G. C. Kim, M. Y. Hassan, and S. O. Fadhl, "Operation and control strategies of integrated distributed energy resources: A review," *Renewable and Sustainable Energy Reviews*, vol. 51, pp. 1412–1420, Nov. 2015.

[3] S. M. Kaviri, M. Pahlevani, P. Jain, and A. Bakhshai, "A review of AC microgrid control methods," *IEEE 8th International Symposium on Power Electronics for Distributed Generation Systems (PEDG)*, pp. 1–8, 2017.

[4] Y. Yoldaş, A. Önen, S. M. Muyeen, A. V. Vasilakos, and İ. Alan, "Enhancing smart grid with microgrids: Challenges and opportunities," *Renewable and Sustain. Energy Rev.*, vol. 72, pp. 205–214, May 2015.

[5] M. A. Zamani, A. Yazdani, and T. S. Sidhu, "A control strategy for enhanced operation of inverter-based microgrids under transient disturbances and network faults," *IEEE Trans. Power Syst.*, vol. 27, no. 4, pp. 1737–1747, Oct. 2012.

[6] J. D. Park and J. Candelaria, "Fault detection and isolation in low-voltage DC-bus microgrid system," *IEEE Trans. Power Del.*, vol. 28, no.2, pp. 779–787, Apr. 2013.

[7] H. J. Laaksonen, "Protection Principles for Future Microgrids," *IEEE Trans. Power Electron.*, vol. 25, no.12, pp. 2910–2918, Dec. 2010.

[8] M. Aldeen and R. Sharma, "Robust detection of faults in frequency control loops," *IEEE Trans. Power Syst.*, vol. 22, no. 1, pp. 413–422, Feb. 2012.

[9] F. Caliskan and I. Genc, "A robust fault detection and isolation method in load frequency control loops," *IEEE Trans. Power Syst.*, vol. 23, no. 4, pp. 1756–1767, Nov. 2008.

[10] S. Gholami, S. Saha, and M. Aldeen, "Sensor fault tolerant control of microgrid," *IEEE Power Energy Soc. Gen. Meeting (PESGM)*, pp. 1–5, 2016.

[11] S. Gholami, S. Saha, and M. Aldeen, "Fault tolerant control of electronically coupled distributed energy resources in microgrid systems," *International Journal of Electr. Power & Energy Syst.*, vol. 95, pp. 327–340, Feb. 2018.

[12] M. E. Raoufat, K. Tomsovic, and S. M. Djouadi, "Virtual actuators for wide-area damping control of power systems," *IEEE Trans. Power Syst.*, vol. 31, no. 6, pp. 4703–4711, Nov. 2016.

[13] J. T. Allen and N. H. El-Farra, "A model-based framework for fault estimation and accommodation applied to distributed energy resources," *Renewable Energy*, vol. 100, pp. 35–43, Jan. 2017.

[14] J. Lunze, "From fault diagnosis to reconfigurable control: A unified concept," *3rd IEEE Control and Fault-Tolerant Syst. (SysTol)*, pp. 413–421, 2016.

[15] J. H. Richter, "Reconfigurable Control on Nonlinear Dynamical Systems: A Fault-Hiding Approach," *Springer-Verlag*, 2011.

[16] J. Lunze, S. Pröll, and F. Jarmolowitz, "From structural analysis to observer-based residual generation for fault detection," *IEEE Control and Fault-Tolerant Systems Conference (SysTol)*, pp. 491–498). Sep. 2016.